International Journal of Science and Research (IJSR)
ISSN (Online): 2319-7064
Index Copernicus Value (2013): 6.14 | Impact Factor (2013): 4.438

Parametric Significance of Warm Drawing Process for 2024T4 Aluminum Alloy through FEA

A. Chennakesava Reddy

A. Chennakesava Reddy, Professor, Department of Mechanical Engineering, JNT University, Hyderabad-500 085, India

Abstract: ***In this present work, a statistical approach based on Taguchi Techniques and finite element analysis were adopted to determine the parametric significance on the formability of cup using warm drawing process. The process parameters were thickness of blank, temperature, coefficient of friction and strain rate. The thickness of sheet, coefficient of friction and strain rate have been found influencing the quality of the cup drawn from 2024T4 aluminum alloy.***

Keywords: 2024 Al alloy, warm drawing process, thickness, temperature, coefficient of friction, strain rate, finite element analysis.

1. Introduction

Many investigations have been carried out to obtain an optimal blank shape that can be deformed into the near-net shape. Chung et al. [1] have proposed a direct design method based on an ideal forming theory to get an initial blank shape. But real forming conditions such as blank holder force, friction force, tool geometry are not considered. Shehata et al. [2] have demonstrated the formability can be improved using differential temperature rather than a uniform temperature rise. Finch et al. [3] investigated the effect of warm forming on drawability of both rectangular and circular cups from annealed and hardened aluminum sheet alloys. The results indicated significant improvement in the drawability in terms of cup height at a temperature of about 150^{0}C even for the precipitation hardened alloys (like 2024-T4 and 7075-T6). Toros et al. [4] have developed an analytical model to evaluate deep drawing process at elevated temperatures and under different blank holder pressure (BHP) and identified that blank temperature; punch speed, BHP, and friction are the main factors that influence formability. Jeyasingh et al. [5] have carried out investigations on failures of hydroforming deep drawing processes. The punch deforms the blank to its final shape by moving against a controlled pressurized fluid, which acts hydrostatically via a thin rubber diaphragm. As a result of the controllable backup pressure, a favorable pressure path, with respect to the punch travel, can be sought in order to delay the premature failures. The failure by rupture results from an excessive fluid pressure, while wrinkling results from insufficient fluid pressure. The range of pressure in between these two boundaries, give the working zone. Reddy et al. [6] have carried out the experimental characterization on the warm deep drawing process of extra-deep drawing (EDD) steel. The results of the experimentation conclude that the extent of thinning at punch corner radius is lower in the warm deep-cup drawing process of EDD steel at 200^{0}C. Reddy et al. [7] in another work have simulated that the cup drawing process with an implicit finite element analysis. The effect of local thinning on the cup drawing has been investigated. The thinning is observed on the vertical walls of the cup. The strain is maximum at the thinner sections. Reverse superplastic blow forming of a Ti-6Al-4V sheet has been simulated using finite element method to achieve the optimized control of thickness variation [8]. Reddy [9] has used Taguchi technique which can save the cost of experimentation to optimize the extrusion process of 6063 aluminum alloy.

Grain boundary nucleation has been frequently observed and it plays a dominant role in recrystallization kinetics when the initial grain size is small, or at lower strains [10]. The second inhomogenity refers to the fact that the deformation microstructures varies from grain to grain because of the initial crystallographic texture. As a result, the nucleation sites for recrystallization in deformed grains with different orientations are different [11]. Each as-deformed grain will recrystallize at a rate that depends on its size as well as initial orientation with respect to the deformation field depending on the accumulation of the stored energy. Although many investigators have developed mathematical models to predict the temperature distribution and the strain distribution of the slab during hot rolling [12], very few publications paid attention to the deformation history and the variation of the strain rate pattern during hot rolling, which have been recognized as two important parameters for hot deformation. In practical hot rolling conditions, where the nominal strain rate ranges from 0.1 to 100 /s, the yield stress characteristics of the material are strain rate rather than strain dependent. 2024A is an aluminum alloy, with copper as the primary alloying element. It is used in applications requiring high strength to weight ratio, as well as good fatigue resistance. With its relatively good fatigue resistance, especially in thick plate forms, alloy 2024 continues to be specified for many aerospace structural applications. Alloy 2024 plate products are used in fuselage structural, wing tension members, shear webs and ribs and structural areas where stiffness, fatigue performance and good strength are required.

The objective of the present work is to optimize the warm deep drawing process of 2024A aluminum alloy using Taguchi technique. In this present work, a statistical approach based on Taguchi techniques was adopted to determine the degree of importance of each of the process parameter on the formability of deep drawn cup. D-FORM software was used to develop warm deep drawing process for 2024 aluminum alloy.

2. Materials and Methods

2024T4 aluminum alloy was used to fabricate deep drawing cups. The tensile and yield strengths of this alloy are 469 and

324 MPa respectively. The elastic modulus is 73.1 GPa. The Poisson's ratio is 0.33. The percent elongation is 20% of 1.2 mm sheet thickness) . The shear strength is 283 MPa. The control parameters are those parameters that a manufacturer can control the design of the product, and the design of process. The levels chosen for the control parameters were in the operational range of 2024T4 aluminum alloy using deep drawing process. Each of the three control parameters was studied at three levels. The chosen control parameters are summarized in table 1.

Table 1: Control parameters and levels

Factor	Symbol	Level–1	Level–2	Level–3
Thickness, mm	A	0.80	1.00	1.20
Temperature, ^{0}C	B	300	400	500
Coefficient of Friction	C	0.20	0.30	0.40
Strain rate	D	1	25	50

The orthogonal array (OA), L9 was selected for the present work. The parameters were assigned to the various columns of O.A. The assignment of parameters along with the OA matrix is given in table 2. 2024T4 aluminum alloy sheets were subjected to a homogenization treatment in a laboratory air furnace with controlled heating rates. All the sheets were annealed at 300, 400 and 500°C for a period of 8 hrs. Microstructural examination of the heat treated samples was also carried out using optical microscope.

Table 2: Orthogonal array (L9) and control parameters

Treat No.	A	B	C	D
1	1	1	1	1
2	1	2	2	2
3	1	3	3	3
4	2	1	2	3
5	2	2	3	1
6	2	3	1	2
7	3	1	3	2
8	3	2	1	3
9	3	3	2	1

2.1 Fabrication of Deep Drawn Cups

The blank size was calculated by equating the surface area of the finished drawn cup with the area of the blank. The diameter meter of the blank is given by:

$$D = \sqrt{d^2 + 4dh} \text{ for } d/r > 20 \qquad (1)$$

$$D = \sqrt{d^2 + 4dh} - 0.5r \text{ for } 20 < d/r < 20 \qquad (2)$$

$$D = \sqrt{d^2 + 4dh} - r \text{ for } 15 < d/r < 10 \qquad (3)$$

$$D = \sqrt{(d - 2r)^2 + 4d(h - r) + 2\pi r(d - 0.7r)} \text{ for } 2d/r < 10 \qquad (4)$$

where d is the mean diameter of the cup (mm), h is the cup height (mm) and r is the corner radius of the die (mm).

The force required for drawing depends upon the yield strength of the material σ_y, diameter and thickness of the cup:

$$\text{Drawing force, } F_d = \pi dt[D/d - 0.6]\sigma_y \qquad (5)$$

where D is the diameter of the blank before operation (mm), d is the diameter of the cup after drawing (mm), t is the thickness of the cup (mm) and σ_y is the yield strength of the cup material (N/mm^2).

The drawing punches must have corner radius exceeding three times the blank thickness (t). However, the punch radius should not exceed one-fourth the cup diameter (d).

$$3t < \text{Punch radius} < d/4 \qquad (6)$$

For smooth material flow the die edge should have generous radius preferably four to six times the blank thickness but never less than three times the sheet thickness because lesser radius would hinder material flow while excess radius the pressure area between the blank and the blank holder, and would cease to be under blank pressure. The corner radius of the die can be calculated from the following equation:

$$r = 0.8\sqrt{(D - d)t} \qquad (7)$$

The drawing ratio is roughly calculated as

$$DR = D/d \qquad (8)$$

The material flow in drawing may render some flange thickening and thinning of walls of the cup inevitable. The space for drawing is kept bigger than the sheet thickness. This space is called die clearance.

$$\text{Clearance, } c = t + \mu\sqrt{10t} \qquad (9)$$

The sheets of 2024 aluminum alloy were cut to the required blank size. The blank specimens were heated in a muffle furnace to the desired temperature as per the design of experiments. The blank pressure was calculated, as in (5). The cups were fabricated using hydraulically operated deep drawing machine as shown in figure 1.

3. Finite Element Modeling and Analysis

The finite element modeling and analysis was carried using D-FORM 3D software. The circular sheet blank was created with desired diameter and thickness. The cylindrical top punch, cylindrical bottom hollow die were modeled with appropriate inner and outer radius and corner radius [13]. The clearance between the punch and die was calculated as in (9). The sheet blank was meshed with tetrahedral elements [14]. The modeling parameters of deep drawing process were as follows:

Number of elements for the blank: 21032 tetrahedron
Number of nodes for the blank: 7218
Top die polygons: 9120
Bottom die polygons: 9600.

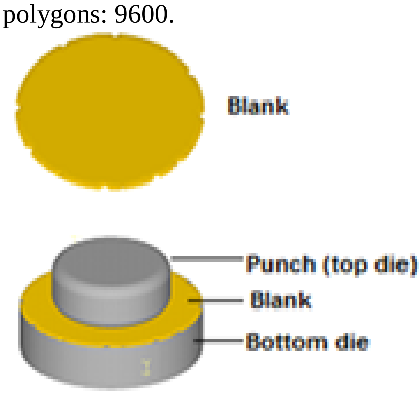

Figure 1: Initial position die, punch and

The initial position of the die, blank and punch is shown in figure 1. The contact between blank and punch, die and blank holder were coupled as contact pair. The mechanical interaction between the contact surfaces was assumed to be frictional contact. The finite element analysis was chosen to find the effective stress, effective strain, volume of the cup, and damage of the cup. The finite element analysis was conceded to run using D-FORM 3D software according to the design of experiments for the purpose of validating the results of experimentation.

4. Results and Discussion

The experiments were scheduled on random basis to accommodate the manufacturing impacts (like variation of temperature, pressure). Two trials were carried out for each experiment. The sheet thickness of the tensile test specimen was 1.2 mm. The true tensile strength decreases with an increase in the strain rate as shown in figure 2.

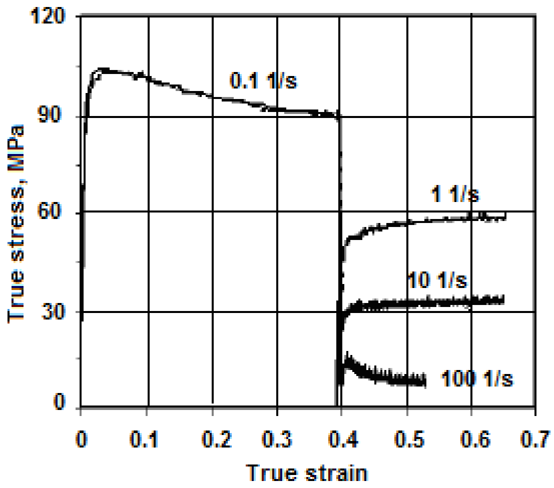

Figure 2: True stress-strain of 2024A alloy at 400^{0}C.

4.1 Influence of process parameters on effective Stress

Table 3 gives the ANOVA (analysis of variation) summary of raw data. The Fisher's test column establishes all the parameters (A, B, C and D) accepted at 90% confidence level. The percent contribution indicates that the thickness parameter, A puts in 6.05% of variation, B (temperature) supports 30.39% of variation, C (coefficient of friction) influences 13.16% of variation and D (strain rate) contributes 50.35% of variation on the effective tensile stress.

Table 3: ANOVA summary of the effective stress

Source	Sum 1	Sum 2	Sum 3	*SS*	*v*	*V*	*F*	*P*
A	1295.8	1073	1043.5	6342.53	2	3171.27	148.82	6.05
B	1486	1029.5	896.8	31842.13	2	15921.06	747.12	30.39
C	1010.5	1372	1029.8	13786.43	2	6893.21	323.47	13.16
D	1354	1380	678.3	52757.2	4	13189.3	618.93	50.35
Error				21.31	7	3.04	0.14	0.05
T	5146.3	4854.5	3648.4	104749.6	17			100

Note: Note: SS is the sum of square, v is the degrees of freedom, V is the variance, F is the Fisher's ratio, P is the percentage of contribution and T is the sum squares due to total variation.

The influence of thickness on the effective stress is shown figure 3. The effective stress of the cups decreases from 215.97 to 173.92 MPa with increasing thickness of sheet from 0.8 to 1.2 mm. This is practical as the denominator component of 'stress = force/area' increases the stress value decreases. Thin sheets of 0.8 mm and 1.0 mm were damaged due to high induced stress in the blank material during warm deep drawing operations. The cups (with less damage) were drawn with thick sheets of 1.2 mm wherein low stress value was developed in the blank material.

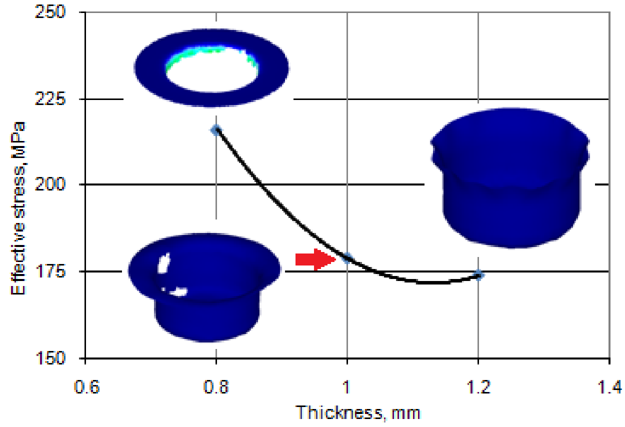

Figure 3: Influence of sheet thickness on the effective stress.

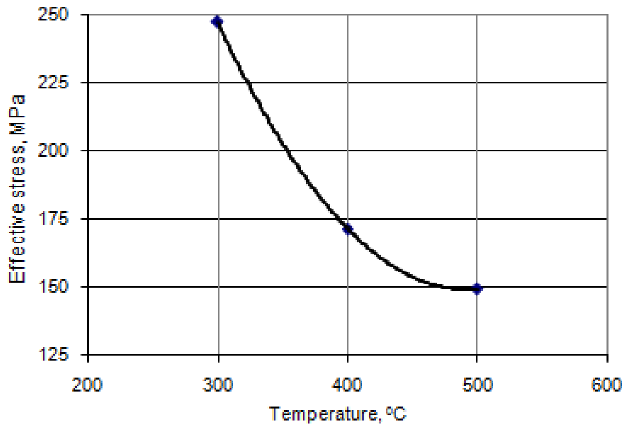

Figure 4: Influence of temperature on the effective stress.

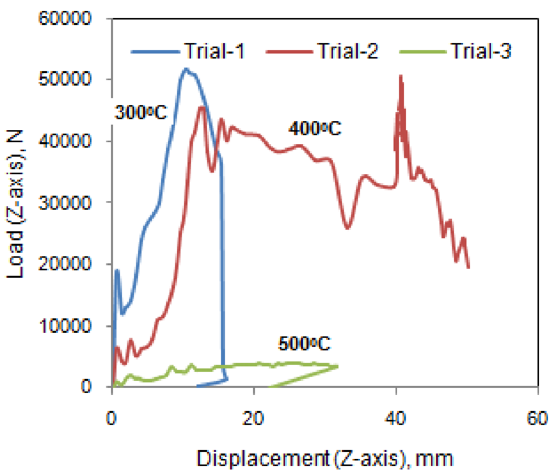

Figure 5: Influence of temperature on the load.

The effective stress decreases from 114.65 to 64.46 MPa with increasing temperature from 300 to 500^{0}C (figure 4). This is owing to the softening of material with an increase in the temperature. The maximum forming load decreases as the working temperature is increased. For instance, the maximum forming load is found to decrease from 52KN to 40KN over the working temperature range 300^0C ≤ T ≤ 500 ^{0}C for the blank thickness of 0.8mm under trails 1to3 as shown in figure 5. The influence of friction coefficient on the effective stress is shown in figure 6. It is found that the effective stress is maximum for the friction coefficient of 0.3.

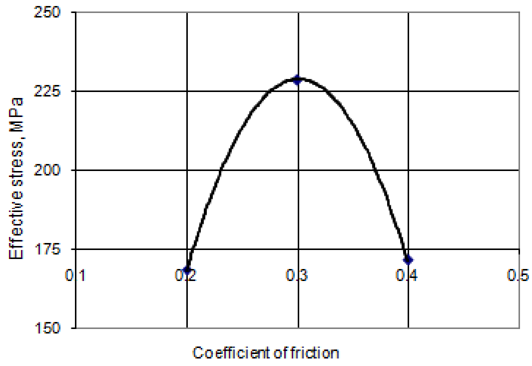

Figure 6: Influence of temperature on the effective stress

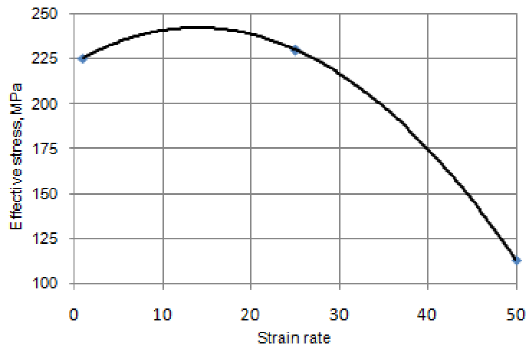

Figure 7: Influence of strain rate on the effective stress

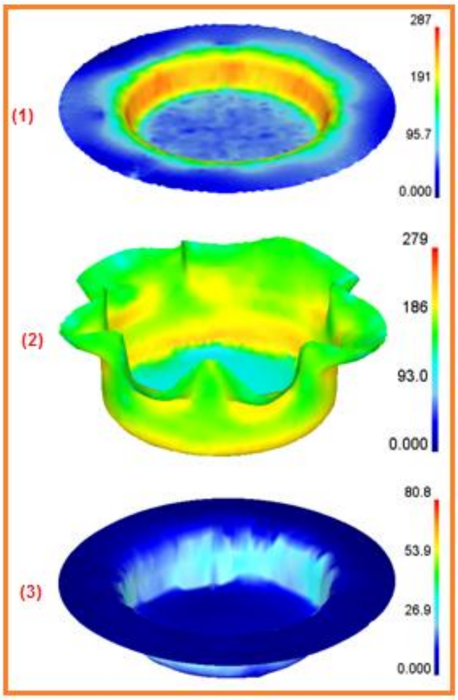

Figure 8: Influence of process parameters on the effective stress for blank thickness of 0.8 mm

The influence of strain rate on the effective stress is shown in figure 7. It is observed that the effective stress decreases with an increase in the strain rate. This phenomenon can also be confirmed from figure 2 that the true stress decreases with an increase in the strain rate.

.

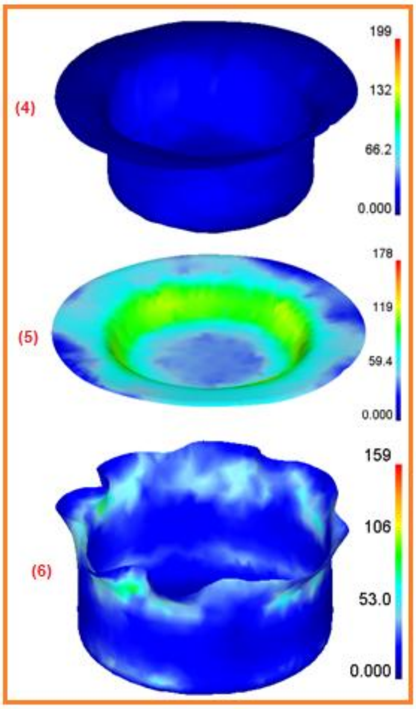

Figure 9: Influence of process parameters on the effective stress for blank thickness of 1.0 mm

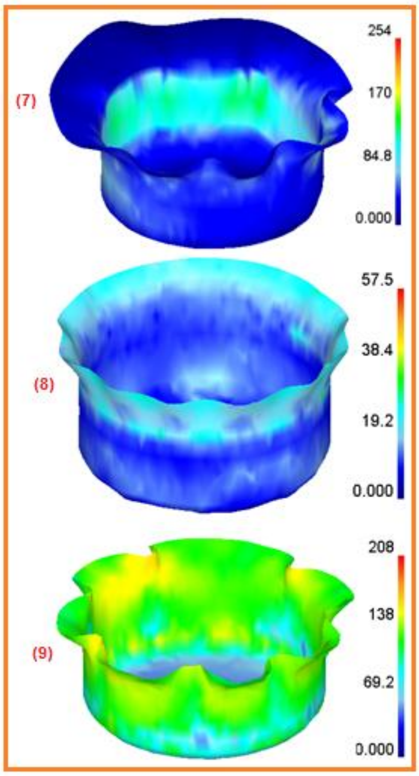

Figure 10: Influence of process parameters on the effective stress for blank thickness of 1.2 mm

The FEA results of effective stress are shown in figures 8 to 10 for various test conditions as per the design of experiments. It was found that the trail- 8 could give big cup as compared to the rest of test conditions with maximum effective stress of 57.5 MPa which is very much lesser than the yield strength of 324 MPa (at room temperature).

4.2 Influence of process parameters on height of cup

The ANOVA summary of cup height is given in table 4. The Fisher's test column ascertains all the parameters (A, B, C, and D) accepted at 90% confidence level influencing the variation in the flexural strength. The percent contribution indicates that thickness of sheet gives 31.49%of variation, coefficient of friction contributes 17.27% of variation and strain rate controls 46.55% of variation. The influence of temperature is negligible.

Table 4: ANOVA summary of the height of cup

Source	Sum 1	Sum 2	Sum 3	*SS*	*v*	*V*	*F*	*P*
A	186.4	233.7	297.6	1038.12	2	519.06	10.06	31.49
B	240.3	227.5	249.9	42.11	2	21.06	0.41	0.84
C	256.6	269.3	191.8	575.93	2	287.97	5.58	17.27
D	160.7	279.6	277.4	1542.28	4	385.57	7.47	46.55
Error				51.58	7	7.37	0.14	3.85
T	844	1010.1	1016.7	3250.02	17			100

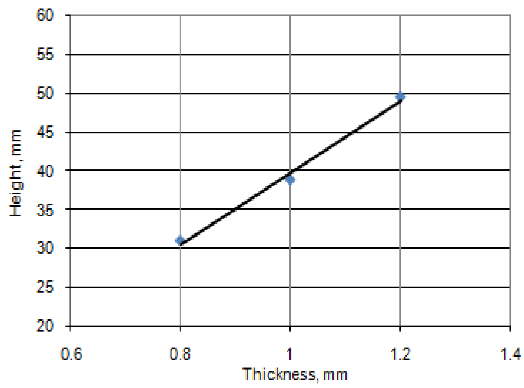

Figure 11: Influence of sheet thickness on the height of cup

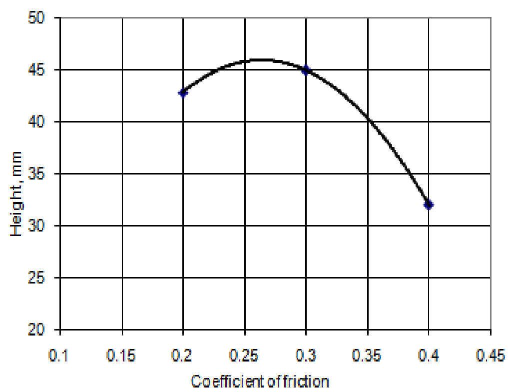

Figure 12: Influence of friction on the height of cup

The height of cup increases with an increase in the thickness of sheet as shown in figure 11. The height of the cup decreases with an increase in the coefficient of friction from 0.3 to 0.4(figure 12). The height of the cup decreases with an increase in the strain rate (figure 13).

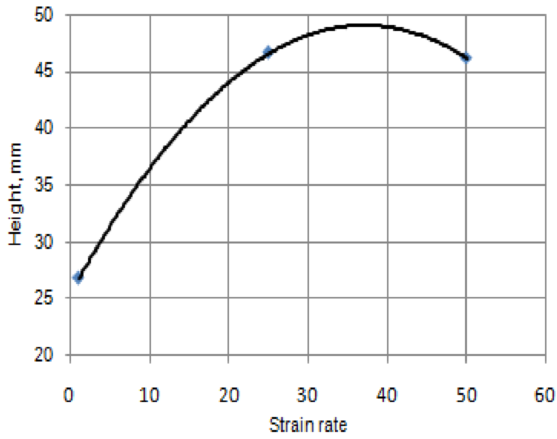

Figure 13: Influence strain rate on the height of cup

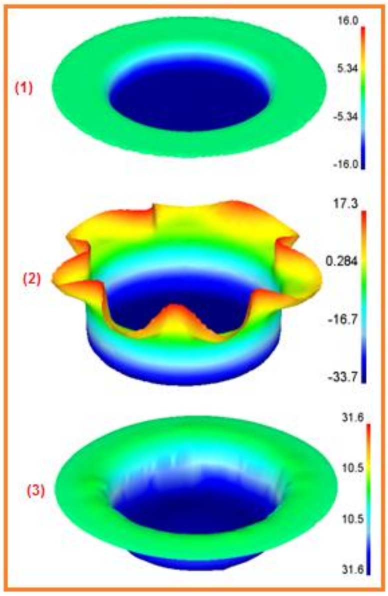

Figure 14: FEA results showing the heights of cups for blank thickness of 0.8 mm

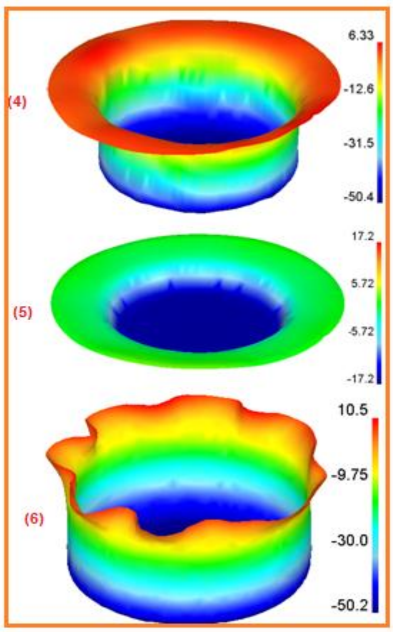

Figure 15: FEA results showing the heights of cups for blank thickness of 1.0 mm

International Journal of Science and Research (IJSR)
ISSN (Online): 2319-7064
Index Copernicus Value (2013): 6.14 | Impact Factor (2013): 4.438

The FEA results of the cups drawn with different trials as per the design of experiments are shown in figures 14 to 16. The target height of the cup was 50 mm with diameter 100 mm. More than the expected cup height (56.8 mm) was reached for trail 8.

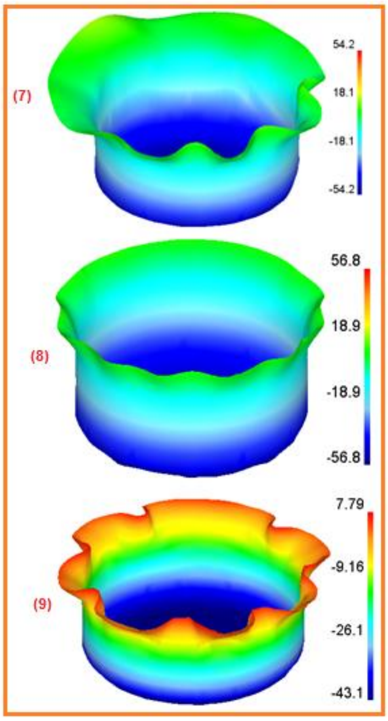

Figure 16: FEA results showing the heights of cups for blank thickness of 1.2 mm

4.3 Influence of process parameters on damage of cup

The ANOVA summary of damage of cups is given in table 5. The Fisher's test column ascertains the parameters (A, B, C and D) accepted at 90% confidence level influencing the variation in the cup height. The percent contribution indicates that the thickness of the sheet only contributes half (56.01%) of the variation, parameter, B (temperature) aids 3.03% of variation, coefficient of friction (C) contributes 26.94% of variation and strain rate (D) contributes 13.22% of variation.

Table 5: ANOVA summary of the damage of cup

Source	Sum 1	Sum 2	Sum 3	*SS*	*v*	*V*	*F*	*P*
A	56.32	19.78	7.65	213.95	2	106.98	86.16	56.01
B	21.78	28.24	33.73	11.93	2	5.97	4.81	3.03
C	7.86	35.19	40.7	103.1	2	51.55	41.52	26.94
D	15.25	28.5	40	51.14	4	12.79	10.30	13.22
Error				1.24	7	0.18	0.15	0.8
T	101.21	111.71	122.08	381.36	17			100

The effect of thickness on the damage of cup is shown in figure 17. The damage decreases with an increase in the thickness of the sheet. The average distribution of the blank thinning increases with an increase in the blank thickness. Ironing can be defined as thinning of the blank at the die cavity. The main reasons for the damage of cups were due to ironing and the coefficient of friction. The clearance was obtained by the formula as in eq. (9).

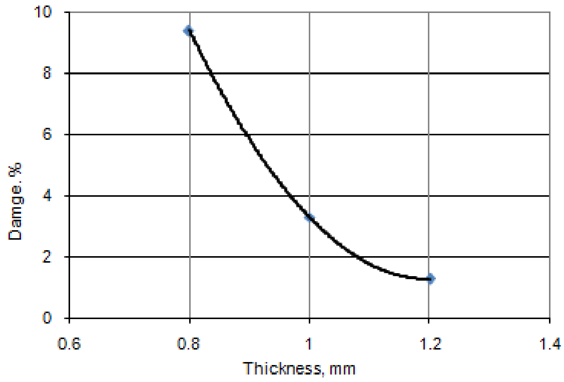

Figure 17: Influence of thickness on the damage of cup.

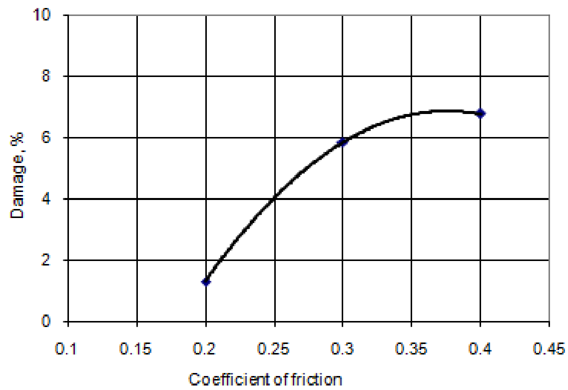

Figure 18: Influence friction on the damage of cup.

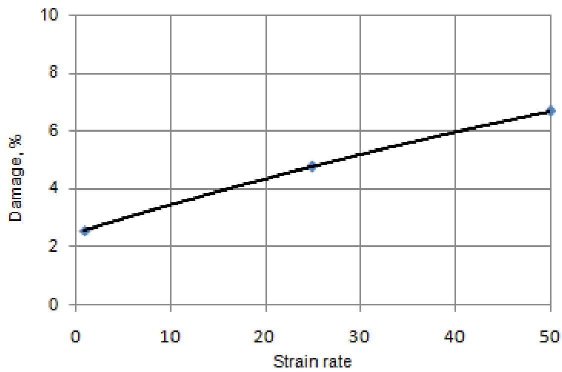

Figure 19: Influence of strain rate on the damage of cup.

In the case of friction between the piece and the tool, the increase of the coefficient of friction determines the wrinkling to reduce, but high values of the coefficient can cause cracks (figure 18) and material breakage. In the case of deep-drawing, under the effect of the deformation force, the blank is subjected to a tangential compression stress and a radial extension stress. For instance, in the case of the thin sheets, although the radial extension stress of the flange is relatively high, the tangential compression stress can lead to the risk of its wrinkling, a risk which is very likely to appear when the difference between the outer diameters of the blank and the finished piece is big and the sheet thickness is small. It is observed form figure 18 that the damage in the cup increases with an increase in the coefficient of friction from 0.2 to 0.4. It was observed that if the friction forces are low, the wrinkling is more pronounced, but if the friction forces are too high the material can break. The optimum value of friction coefficient could be 0.2. The damage in the cups increases with an increase in the strain rate as shown in figure 18. The damages were 2.54, 4.75 and 6.67 for the strain rates of 1, 25 and 50 respectively. It is observed from 20 that there was no damage of the cup drawn with process parameters of trial 8.

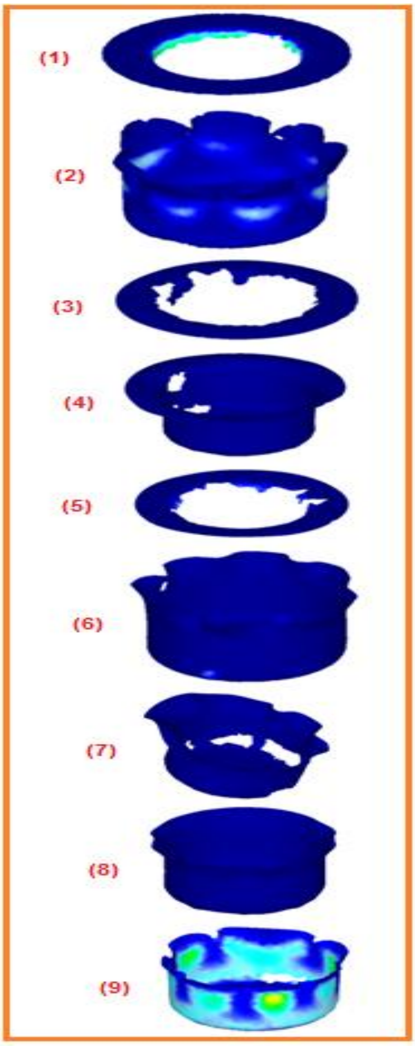

Figure 19: Influence of process parameters on the damage of cup.

5. Conclusions

The finite element analysis of warm drawing of 2024T4 aluminum alloy was carried out. It was observed that sheet thickness, coefficient of friction and strain rate were highly significant to obtain the required dimensional cup. The best significant process parameters are sheet thickness of 1.2 mm, temperature of 400^0C, friction coefficient of 0.2 and strain rate of 50 1/s.

6. Acknowledgment

The author wishes to thank University Grants Commission (UGC), New Delhi, India for financial assisting this project.

References

[1] K. Chung, F.Barlat and J.C. Brem, "Blank shape design for a planar anisotropy sheet based on ideal forming design theory and FEM analysis," International Journal of Mechanical Sciences, 39, pp.617–633, 1997.

[2] F. Shehata, M.J. Painter, and R. Pearce., "Warm forming of aluminum/magnesium alloy sheet," Journal of Mechanical Working Technology, .2, no.3, pp. 279-291, 1978.

[3] D.M. Finch, S.P. Wilson and J.E. Dorn, "Deep drawing aluminum alloys at elevated temperatures. Part II. Deep drawing boxes," Transactions ASM, vol.36, pp. 290–310, 1946.

[4] S. Toros S, F.Ozturk and Ilyas Kacar, "Review of warm forming of aluminum–magnesium alloys," Journal of Materials Processing Technology, vol.207, no.1-3, pp. 1–12, 2008.

[5] J.V.Jeysingh, B. Nageswara Rao , A. Chennakesava Reddy, "Investigation On Failures Of Hydroforming Deep Drawing Processes," Materials Science Research Journal, vol.2, no.3&4, pp.145-168, 2008.

[6] A. Chennakesava Reddy ,T. Kishen Kumar Reddy, M. Vidya Sagar, "Experimental characterization of warm deep drawing process for EDD steel," International Journal of Multidisciplinary Research & Advances in Engineering, vol.4, no.3, pp.53-62, 2012.

[7] A. Chennakesava Reddy, "Evaluation of local thinning during cup drawing of gas cylinder steel using isotropic criteria," International Journal of Engineering and Materials Sciences, vol.5, no.2, pp.71-76, 2012.

[8] A. Chennakesava Reddy, "Finite element analysis of reverse superplastic blow forming of Ti-Al-4V alloy for optimized control of thickness variation using ABAQUS," Journal of Manufacturing Engineering, vol.1, no.1, pp. 06-09, 2006.

[9] A. Chennakesava Reddy, "Optimization of Extrusion Process of Alloy 6063 Using Taguchi Technique," International Journal of Multi- Disciplinary Research & Advances in Engineering, vol.3, no.2, pp.173-190, 2011.

[10] P.L. Orsettirossi and C.M. Sellars, Journal of Material Science and Technology, 15, 185-1921999.

[11] E.C.W. Perryman, Transactions AIME, Journal of Metals, 203, 369-378, 1955.

[12] R. Colas, "Modeling heat transfer during hot rolling of steel strip," Modeling and Simulation in Material Science Engineering, 3, 437-453, 1955.

[13] Chennakesava R Alavala, CAD/CAM: Concepts and Applications, PHI Learning Pvt. Ltd., New Delhi, 2008.

[14] Chennakesava R Alavala, Finite Element Methods: Basic Concepts and Applications, PHI Learning Pvt. Ltd., New Delhi, 2008.